Journal of Applied Polymer Science

# Synthesis of Poly(butyl acrylate)—Laponite Nanocomposite Nanoparticles for Improving the Impact Strength of Poly(lactic acid)

**Yuan Fang,[1] Sandrine Hoppe,[2] Guo-Hua Hu,[1] Alain Durand[2]**

[1]CNRS-Universté de Lorraine, Laboratoire Réactions et Génie des Procédés, UPR3349, ENSIC, 1 rue Grandville, BP 20451, Nancy, F-54000, France

[2]CNRS-Universté de Lorraine, Laboratoire de Chimie Physique Macromoléculaire, UMR 7568, 1 rue Grandville, BP 20451, Nancy, F-54000, France

Correspondence to: H. H. Hu (E-mail: guo-hua.hu@univ-lorraine.fr)

**ABSTRACT:** This work aims at preparing and characterizing poly(butyl acrylate) (PBA)—laponite (LRD) nanocomposite nanoparticles and nanocomposite core (PBA-LRD)-shell poly(methyl methacrylate) (PMMA) nanoparticles, on the one hand, and the morphology and properties of poly(lactic acid) (PLA)-based blends containing PBA-LRD nanocomposite nanoparticles or (PBA-LRD)/PMMA core–shell nanoparticles as the dispersed phase, on the other hand. The PBA and (PBA-LRD)/PMMA nanoparticles were synthesized by miniemulsion or emulsion polymerization using LRD platelets modified by 3-methacryloxypropyltrimethoxysilane (MPTMS). The grafting of MPTMS onto the LRD surfaces was characterized qualitatively using FTIR and quantitatively using thermogravimetric analysis (TGA). The amounts of LRD in the PBA-LRD nanocomposites were characterized by TGA. The PBA/PMMA core–shell particles were analyzed by $^1$H-NMR. Their morphology was confirmed by SEM and TEM. Mechanical properties of (PBA-LRD)/PLA blends and (PBA-LRD)/PMMA/PLA ones were tested and compared with those of the pure PLA, showing that core–shell particles allowed increasing impact strength of the PLA while minimizing loss in Young modulus and tensile strength. © 2013 Wiley Periodicals, Inc. J. Appl. Polym. Sci. 129: 2580–2590, 2013

**KEYWORDS:** biopolymers and renewable polymers; composites; nanoparticles; nanowires; nanocrystals

Received 12 September 2012; accepted 30 December 2012; published online 30 January 2013
**DOI: 10.1002/app.38968**

## INTRODUCTION

In the past decade, poly(lactic acid) (PLA) has attracted much attention because it is biodegradable and is produced from renewable resources. Unfortunately, its impact-strengthened heat resistance are often not satisfactory for many applications.[1–5]

Mineral fillers such as hydroxyapatite, calcium carbonate, calcium phosphate, bamboo fiber, some low molecular weight esters, and plasticizers or rubbers have already been used in combination with PLA to improve its impact strength. Normally impact strength is increased, whereas tensile strength is decreased.[3,5–7]

This work aims at improving the impact strength of PLA while retaining its tensile properties. A classical strategy consists of incorporating both soft elastomers and rigid fillers such as inorganic particulates or glass fibers.[8] Polymer/layered silicate nanocomposites have attracted much attention because they exhibit remarkable enhancement in certain physical and chemical properties compared to conventional composites. It is often necessary to modify pristine clay fillers of hydrophilic nature to increase their compatibility with hydrophobic organic polymers and diminish the tendency of surface-to-surface stacking.[9,10] Several researchers[11–13] have used conventional emulsion polymerization in the presence of hydrophobic agent modified clay platelets to prepare polymer-clay hybrid latex particles. However, clay platelets are only attached on the surfaces of the particles—an armored morphology. By conventional emulsion polymerization procedure, the hydrophobic agent modified-clay particles cannot be incorporated inside polymer particles because they have to go through the water, which is thermodynamically favorable. Miniemulsion polymerization meets the requirements for the encapsulation of hydrophobic clay particles. However, miniemulsions with droplet sizes above 300 nm are often unstable, even in the presence of a sufficient amount of an efficient surfactant. Laponite clay (25 nm in diameter) has been incorporated with monomers via emulison or miniemulsion polymerisation. Generally, synthesis with laponite by emulsion polymerization would also form an armored morphology.[14–16] Besides functionalization by initiators, researches also explored the synthesis of edge modified laponite clay using

alkoxy silane possessing additional reactive groups such as primary amines, methacrylates, benzophenones, monofunctional MPDES, and trifunctional MPTMS. Nanocomposites latexes were then synthesized with laponite functionalized by such silanes,[17–20] and the tensile properties of the resulting nanocomposites were improved with a relatively low solid content.[16]

Wang et al.[21] prepared a core–shell structured complex by seeded emulsion polymerization. The elastomeric core was made of poly(butyl acrylate) (PBA) and the intercalated or exfoliated organophilic montmorillonite (OMMT), and the shell was made of polystyrene (PS). When the core (PBA/OMMT)–shell (PS) structured complex was incorporated in the PS matrix, the impact strength of the PS was improved and its tensile strength retained.

PBA and PLA being immiscible, incorporation of PBA in PLA by simple mixing may likely not be able to improve the impact strength of the latter.[22] On the other hand, it is reported that poly(methyl methacrylate) (PMMA) is partially miscible with and has a higher Young's modulus than PLA, and that its presence in PLA improves the Young's modulus of the latter.[23–25]

The approach developed in this study for improving the impact strength of PLA while retaining as much as possible its tensile strength is to incorporate PBA/laponite nanocomposite latexes in PLA. The laponite particles are functionalized by ion exchange in order to promote polymer formation on their surfaces and create colloidal nanocomposite particles by miniemulsion polymerization. Figure 1 shows the strategy and the reaction steps for the preparation of nanocomposite particles.

## EXPERIMENTAL PART

### Materials

The PLA used was obtained from NaturePLAST (France) in the form of pellets. It had a density of 1.2 g/cm$^3$ and a melt flow index of 2.0–10 g/10 min (190°C/2.16 kg). Its glass transition temperature ($T_g$) and melting temperature ($T_m$) were 48–50°C and 145–155°C, respectively. It was dried in a vacuum oven at 80°C for 3 h before use. Laponite RD® (LRD) was given by Rockwood Additives Ltd. and MPTMS was purchased from ABCR (Germany). All other chemicals were purchased from Sigma-Aldrich and Fluka. Table I shows the materials used for the treatment of laponite particles and the preparation of various polymer particles to be incorporated in the PLA.

### Functionalization

The silylation of the LRD was carried out in toluene. The LRD (6 g) was dried at 60°C for 12 h in a vacuum oven and was added to a flask containing 200 mL of anhydrous toluene. The silylation agent, MPTMS (4.4 g), corresponding to 3 mequiv. of the silylation agent per g of the LRD, was charged to the reaction flask and stirred for several days at 60°C. The resulting LRD (LRD-Si) was extensively washed with toluene to remove the non-grafted silane and dried at 40°C in a vacuum oven overnight for subsequent use.

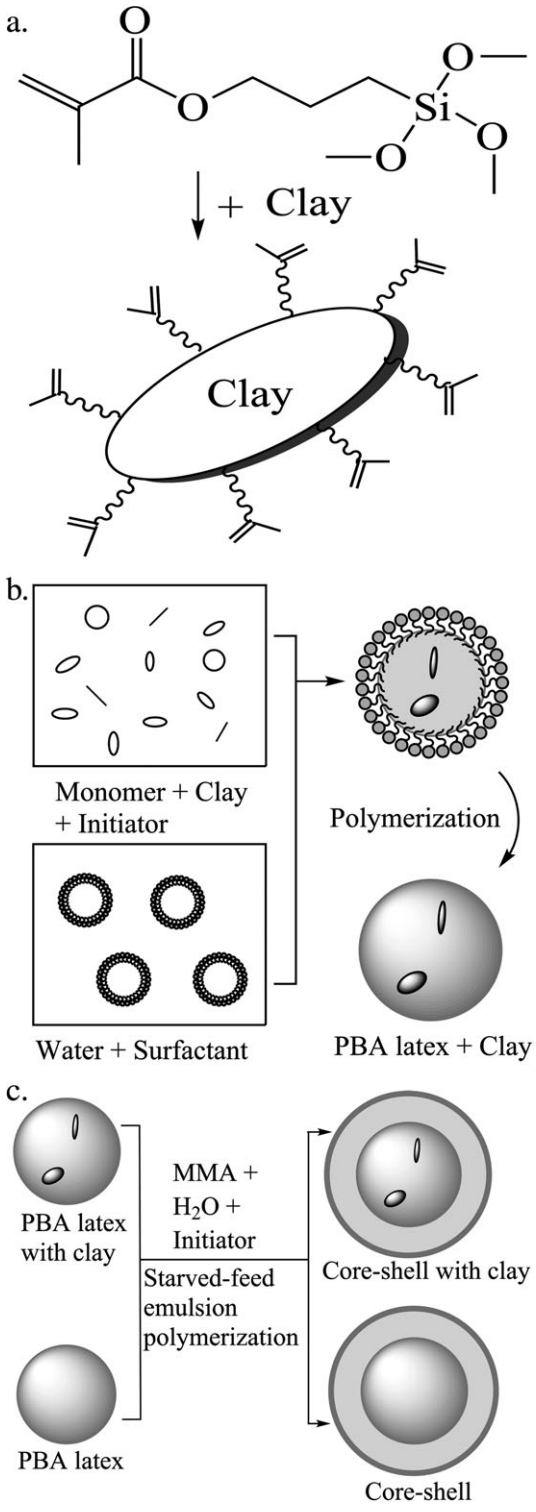


**Figure 1.** Schematic representation of (a) silylation of clay platelets with a tri-functional silane; (b) preparation of PBA/clay composite particles via miniemulsion polymerization; (c) preparation of core (PBA)-shell (PMMA) particles via seeded emulsion polymerization.

### Latex Preparation

Two types of particles were prepared, PBA particles and PBA/PMMA core–shell ones.

**Table I.** Details of the Materials Used for the Treatment of Laponite Particles and the Preparation of Various Types of Polymer Particles

| Material | Formula | Purity | Description | Supplier |
|---|---|---|---|---|
| *n*-Butyl acrylate (BA) | $CH_2$—$CHCOO(CH_2)_3CH_3$ | ≥99% | Monomer | Aldrich |
| Methyl methacrylate (MMA) | $CH_2$—$C(CH_3)COOCH_3$ | ≥99% | Monomer | Fluka |
| 2,2′-Azobis (2-methylbutyronitrile) (AMBN) | $C_{10}H_{16}N_4$ | ≥98% | Initiator | Fluka |
| Hexadecane (HD) | $CH_3(CH_2)_{14}CH_3$ | Anhydrous, ≥99% | Co-stabilizer | Aldrich |
| Laponite RD® (LRD) | $Na^{+0.7}[(Si_8Mg_{5.5}Li_{0.3})O_{20}(OH)_4]^{-0.7}$ | ≤2% water | Clay | Rockwood Additives Ltd. |
| 3-methacryloxypropyltrimethoxysilane (MPTMS) | $C_{10}H_{20}O_5Si$ | >98% | Trifunctional silylation agent | ABCR |
| Toluene | $C_6H_5CH_3$ | ≥99.8% | Solvent | Aldrich |
| Sodium dodecyl sulfate (SDS) | $CH_3(CH_2)_{11}OSO_3Na$ | ≥98.5% | Surfactant | Aldrich |
| Brij 700® | $C_{18}H_{37}(OCH_2CH_2)_{100}OH$ | ≤1% water | Surfactant | Aldrich |
| Brij 78® | $C_{18}H_{37}(OCH_2CH_2)_{20}OH$ | 100% | Surfactant | Aldrich |
| Cetyltrimethylammonium bromide (CTAB) | $CH_3(CH_2)_{15}N(Br)(CH_3)_3$ | ≥99% | Cationic surfactant | Aldrich |
| Octadecyltrimethylammonium bromide (OTAB) | $CH_3(CH_2)_{17}N(Br)(CH_3)_3$ | ≥98% | Cationic surfactant | Aldrich |
| Dimethyldioctadecylammonium chloride (DDAC) | $[CH_3(CH_2)_{17}]_2N(Cl)(CH_3)_2$ | ≥97.0% | Cationic surfactant | Aldrich |
| 2-Butanol | $CH_3CH_2CH(OH)CH_3$ | ≥99.5% | Solvent | Aldrich |

**Synthesis of the PBA Latex Particles.** The PBA latex particles were prepared by miniemulsion polymerization. Table II and Figure 2 show the basic recipes and the miniemulsion polymerization procedure, respectively. The latter was composed of two consecutive steps: preparation of the miniemulsion and polymerization.

***Preparation of the miniemulsion.*** Mixtures A and B were charged to two glass beakers, respectively, under the action of a magnetic bar. After 1 h of magnetic stirring in an ice bath, mixture A was immediately subjected to ultrasonication for 3 min using a sonicator of type Hielscher (0.5 s of cycle time, 70% of amplitude; samples being cooled in an ice bath). Mixture B was prepared with magnetic stirring at room temperature for 1 h, and then cooled in an ice bath. At last, mixtures A and B were mixed together in a glass beaker with magnetic stirring in the ice bath for 30 min and further homogenized with the sonicator in the ice bath for another 3 min. The resulting mixture was ready for the subsequent polymerization.

***Polymerization.*** The as-prepared miniemulsion was first degassed by bubbling with pure nitrogen for 30 min under magnetic stirring in a stainless steel reactor at 20°C. The temperature of the reactor was then raised to 75°C. The polymerization was undertaken at that temperature for more than 3 h with continuous stirring and was terminated by adding hydroquinone to the system. Polymer yields were determined by gravimetry.

**Synthesis of the PBA/PMMA Core–Shell Latex Particles.** The PBA/PMMA core–shell latex particles were prepared by a conventional two-stage emulsion polymerization process. The PBA elastomer core was synthesized according to the recipe shown in Table II. The PMMA rigid shell was synthesized using LRD-PBA latexes or (LRD-Si)-PBA latexes as seeds. Table III shows the recipes for preparing the core–shell composite particles.

The PBA cores prepared by miniemulsion polymerization were further purged with pure nitrogen and under stirring in the stainless steel reactor at 60°C. A mixture of MMA, deionized water, surfactant and AMBN was added to the reactor under starved conditions (0.25 mL/min). After the addition of the monomer mixture, the temperature was raised to 85°C. The reaction proceeded for 3 h under continuous stirring and

**Table II.** Basic Recipes for the Preparation of PBA Latex Particles

| | Mixture A | | | | | | Mixture B | |
|---|---|---|---|---|---|---|---|---|
| Latex PBA | BA (g) | LRD (g) | LRD-Si (g) | CTAB (g) | HD (g) | AMBN (g) | Brij700 or Brij78(g) | $H_2O$ (g) |
| PBA | 20 | – | – | – | 0.8 | 0.4 | 4 | 74 |
| LRD-PBA | 20 | 0.4–1 | – | 0.8 | 0.8 | 0.4 | 4 | 74 |
| (LRD-Si)-PBA | 20 | – | 0.4–1 | 0.8 | 0.8 | 0.4 | 4 | 74 |

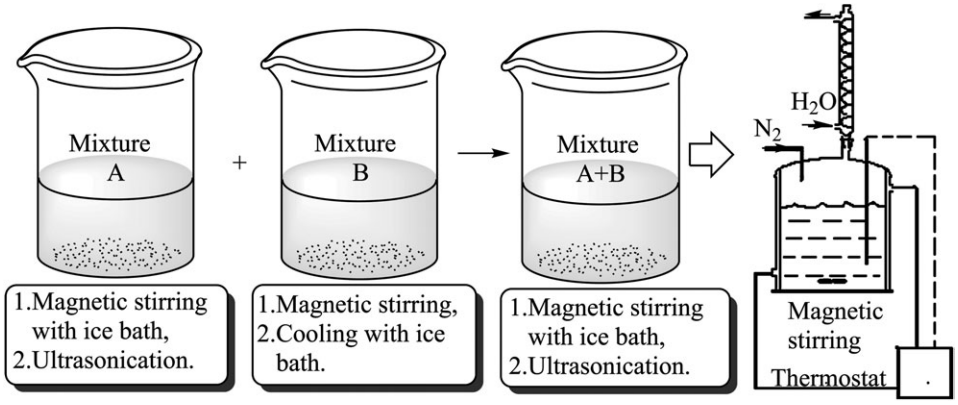


**Figure 2.** Procedure for the preparation of the miniemulsion and its polymerization to obtain PBA latexes.

terminated by the addition of hydroquinone. Polymer yields were determined by gravimetry.

### Preparation of PLA/LRD, PLA/PBA, and PLA/Core–Shell Blends

PBA latexes and PBA/PMMA core–shell ones were demulsified by ethanol and washed with deionized water, then dried at 60°C for 24 h in a vacuum oven before melt blending. The blends of the PLA with dried latexes or with dried LRD particles were prepared in a micro-compounder (DSM Xplore) at a screw speed of 60 rpm for 10 min at 180°C. The neat PLA was subjected to the same mixing treatment so as to have the same thermo-mechanical history as the blends.

### Characterizations

**Infrared, Thermogravimetric, Particle Size, and NMR Analyses.** Infrared spectra were recorded using a Bruker Tensor 27 spectrometer on powder-pressed KBr pellets.

Thermogravimetric analysis (TGA) of the treated clays was performed on a SETRAM Setsys 1200 balance (SETARAM) under nitrogen at a flow rate of 25 $cm^3$/min. Before TGA, the samples were purged with nitrogen. A scanning rate of 10°C/min was used.

The average particle size and particle size distribution were determined by Malvern mastersizer 2000.

NMR spectra were recorded on a Bruker Avance 300 spectrometer equipped at 300 MHz using deuterated chloroform ($CDCl_3$) as a solvent.

**Morphological Observation by Electron Microscopy.** The morphology of the pure PLA and the PLA blends was revealed using scanning electron microscopy of type SEM, JEOL 6490LV. The samples were broken into pieces in liquid nitrogen, sputtered with gold and observed under a working voltage of 8 kV with 800 magnifications.

The morphology of latexes was observed by transmission electron microscopy (TEM) of type Philips CM20 at an acceleration voltage of 200 KV. All latex samples were diluted to 2% solids and treated with negative stain uranyl acetate (2% aqueous solution) in a filtration cell (carbon) with a pore size of 0.2 $\mu$m.

**Mechanical Properties.** Izod impact tests were performed at room temperature with an instrument CEAST Resil Impactor 6967. The specimens (80.5-mm long, 10.5-mm thick, and 4.0-mm wide) were prepared in a hot press at 180°C for 15 min under load.

Tensile properties of the blend samples were measured with a tensile testing machine of type MTS 810 equipped with a video-traction system.[26] The specimens of the PLA with or without LRD, PBA(with or without LRD or LRD-Si)/PLA and (PBA-PMMA)/PLA (with or without LRD or LRD-Si in PBA) were dog bone-like. Their dimensions were 45 mm in length, 5 mm in width, and 4 mm in thickness. The applied crosshead speed was 10 mm/min. Five specimens were tested for each material.

The evolution of seven spots laid on the specimen was monitored in real time by a camera. A computer system recorded the data. An image-software analyzed the variations in distance between the spots and gave access to deformations. The true strain was obtained by summing the deformations in all three directions.

## RESULTS AND DISCUSSION

### Selection of an Adequate Surfactant for Miniemulsion Polymerization

SDS is a classical and efficient anionic surfactant for emulsion as well as miniemulsion polymerization processes. Nevertheless,

**Table III.** Recipes in Weight for the Preparation of PBA/PMMA Latexes

| Latex core-shell | Seed | MMA (g) | MMA/PBA (w/w) | AMBN (g) | Brij700 (g) | $H_2O$ (g) |
|---|---|---|---|---|---|---|
| PBA/PMMA | Latex PBA | 20 | 1 : 1 | 0.2 | 0.9 | 10 |
| LRD-PBA/PMMA | Latex LRD-PBA | 20 | 1 : 1 | 0.2 | 0.9 | 10 |
| (LRD-Si)-PBA/PMMA | Latex (LRD-Si)-PBA | 20 | 1 : 1 | 0.2 | 0.9 | 10 |

preliminary experiments showed that it was not suitable for miniemulsion polymerization in the presence of LRD or LRD-Si. When it was added to the miniemulsion of BA with LRD or LRD-Si, the latex became unstable and exhibited a large amount of sediments (>80 wt % of the initial monomer) after the polymerization.

Unlike SDS, nonionic surfactants like Brij 78 and Brij 700 efficiently stabilized miniemulsions. In addition, their polar head groups containing poly(ethylene oxide) moieties were miscible with PLA.[27] As a result, the latex particles obtained with these two surfactants might have better compatibility with PLA. For the aforementioned reasons, Brij 78 and Brij 700 were chosen as surfactants for the preparation of PBA-LRD composites by miniemulsion polymerization.

Figures 3 and 4 show the change in the size of the PBA latex particles and the corresponding amount of precipitates after the miniemulsion polymerization, respectively, as a function of Brij 700 or Brij 78 content. From Figure 3, the diameter of PBA particles is around 100 nm and the efficiency of the two surfactants is similar. These two figures suggest that both surfactants are effective when their concentrations exceed 4 wt % (weight fraction in the system) and the latexes are stable after the polymerization.

### Hydrophobic Modification of the Laponite

Laponite, a relatively uniform disc-shaped synthetic clay with a diameter of 25 nm and a thickness of 1 nm, appeared to be suitable for being encapsulated by miniemulsion polymerization. The surfaces of the laponite are of hydrophilic in nature and need to be modified to be hydropholic before its dispersion in the BA monomer prior to the miniemulsion polymerization. This step called upon a silylation reaction in toluene ("Experimental" Section). After extensive washing with toluene to eliminate the nonreacted MPTMS coupling agent and drying at 40°C in a vacuum oven overnight, the LRD and LRD-Si powders were characterized by FTIR and TGA.

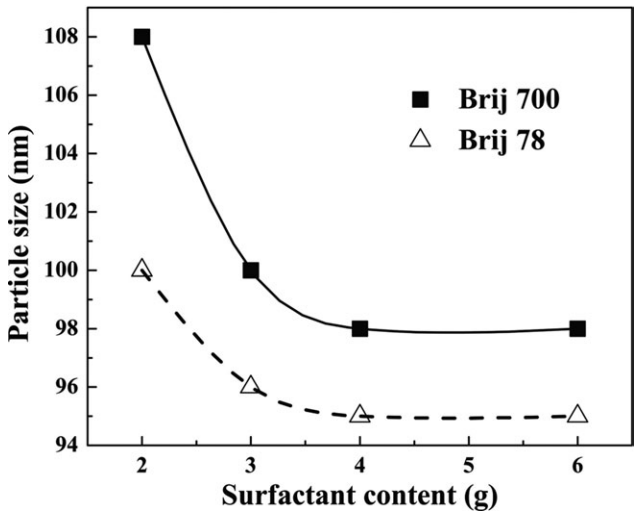


**Figure 3.** Average diameter of final PBA nanoparticles as a function of the amount of Brij 700 or Brij 78 in the feed. The initial amount of BA monomer is 20 g.

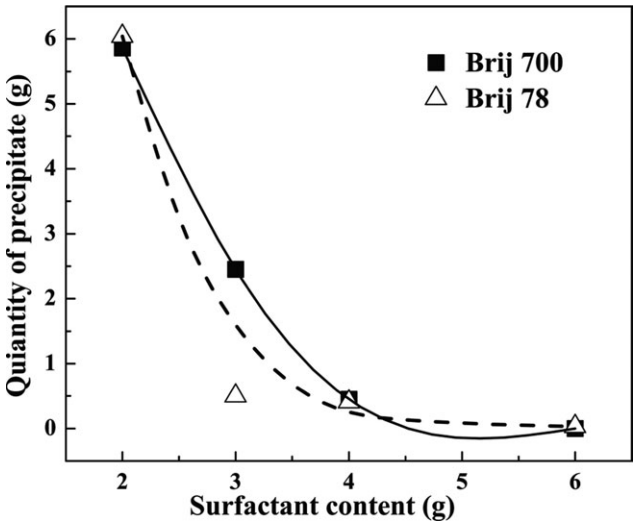


**Figure 4.** Amount of the recovered precipitate after miniemulsion polymerization as a function of the surfactant amount (Brij 700 or Brij 78) in the feed. The amount of BA monomer in the feed is 20 g.

Figure 5 shows the FTIR spectrum of the bare LRD and that of MPTMS grafted LRD denoted as LRD-Si. The bare LRD spectrum exhibits a band at around 3453 $cm^{-1}$, indicating the presence of physisorbed water. This is corroborated by the presence of a band at 1640 $cm^{-1}$ characteristic of the $\upsilon$OH and $\delta$OH deformations. A small shoulder at around 3680 $cm^{-1}$ is due to hydroxyls on the LRD surfaces.

After the grafting of MPTMS onto the LRD, the spectra shows a characteristic vibration of the carbonyl ($\upsilon$C=O, 1703 $cm^{-1}$); the small shoulder at around 3680 $cm^{-1}$ corresponding to the hydroxyl moieties on the LRD surfaces ($Mg_s$-OH) is shifted to 3687 $cm^{-1}$. Moreover, it becomes sharper and increases in intensity. At the same time, the area under the broad band at 3450 $cm^{-1}$ decreases. The existence of residual $Mg_s$-OH in the LRD-Si IR spectra indicates that they are not accessible to the MPTMS silane coupling molecules. The increase in the $Mg_s$-OH band intensity results from a decrease in the amount of physisorbed water after the MPTMS grafting.

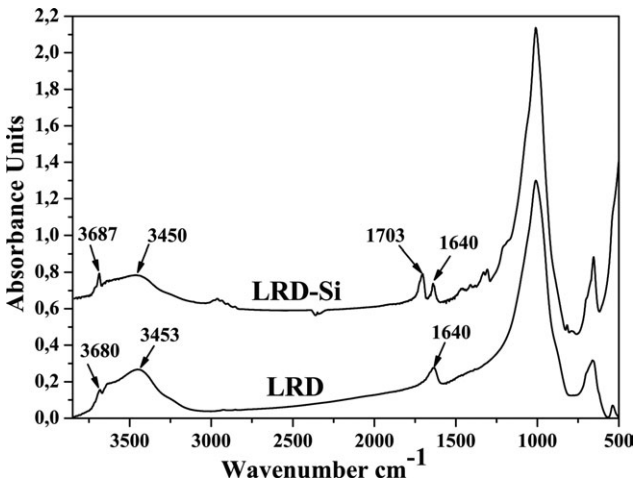


**Figure 5.** FTIR spectra of the bar LRD and MPTMS grafted LRD (LRD-Si)

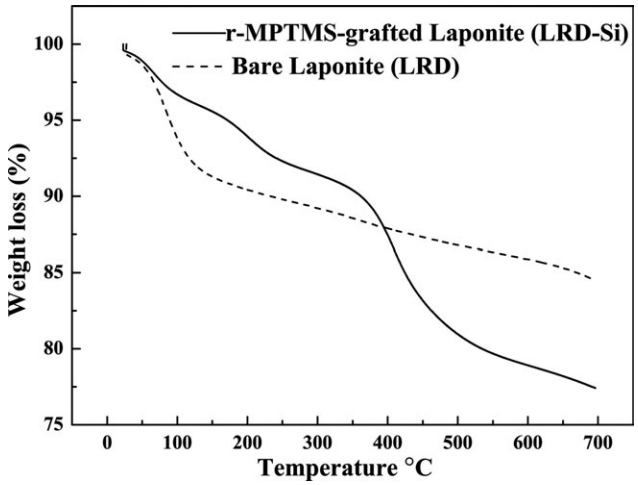


**Figure 6.** TGA traces of the bare LRD and MPTMS-grafted LRD.

TGA is used to evaluate the amount of the silane molecules chemically bonded on the clay edges. Figure 6 shows the TGA curves before and after the grafting of the MPTMS onto the LRD. The region between 200 and 600°C corresponds to the thermal decomposition of the silane moiety.[17] From the TGA curves, the LRD-Si contains approximately 15 wt % MPTMS grafted onto the LRD. For comparison, the reaction feed contained 42 wt % MPTMS. Therefore approximately 24% of MPTMS had reacted.

**Table IV.** Amounts of Precipitates After the Polymerization Without or With a Cationic Surfactant in the Miniemulsion of PBA-3%LRD-Si

| Cationic surfactant (0.8 g) | Without | DDAC | OTAB | CTAB |
|---|---|---|---|---|
| Amount of precipitates (g) | 18.3 | 2.2 | 2.1 | 0.5 |

Initial amounts of BA: 20 g.

### Contribution of Cationic Surfactants to Dispersion of the Laponite in BA

More than 95% of the LRD-grafted (LRD-Si) was precipitated out after the polymerization in the absence of CTAB, OTAB, or DDAC. This is because in the as-prepared mixture prior to miniemulsion polymerization, the dispersion of LRD-Si was not stable without those cationic surfactants. Table IV shows that among those three cationic surfactants, CTAB was the most effective at promoting the dispersion of LRD-Si in BA monomer and avoiding massive sedimentation during miniemulsion polymerization.

### Characterization of PBA Latexes

After the miniemulsion polymerization, TEM was used to examine the latex particle morphology in the wet state. Figure 7 shows representative images of the PBA latexes with LRD or LRD-Si. All the PBA particles remain spherical after the polymerization and their diameter is around 100 nm which is consistent with the average diameters determined by dynamic light scattering (Figure 3). The black line and black disk in Figure

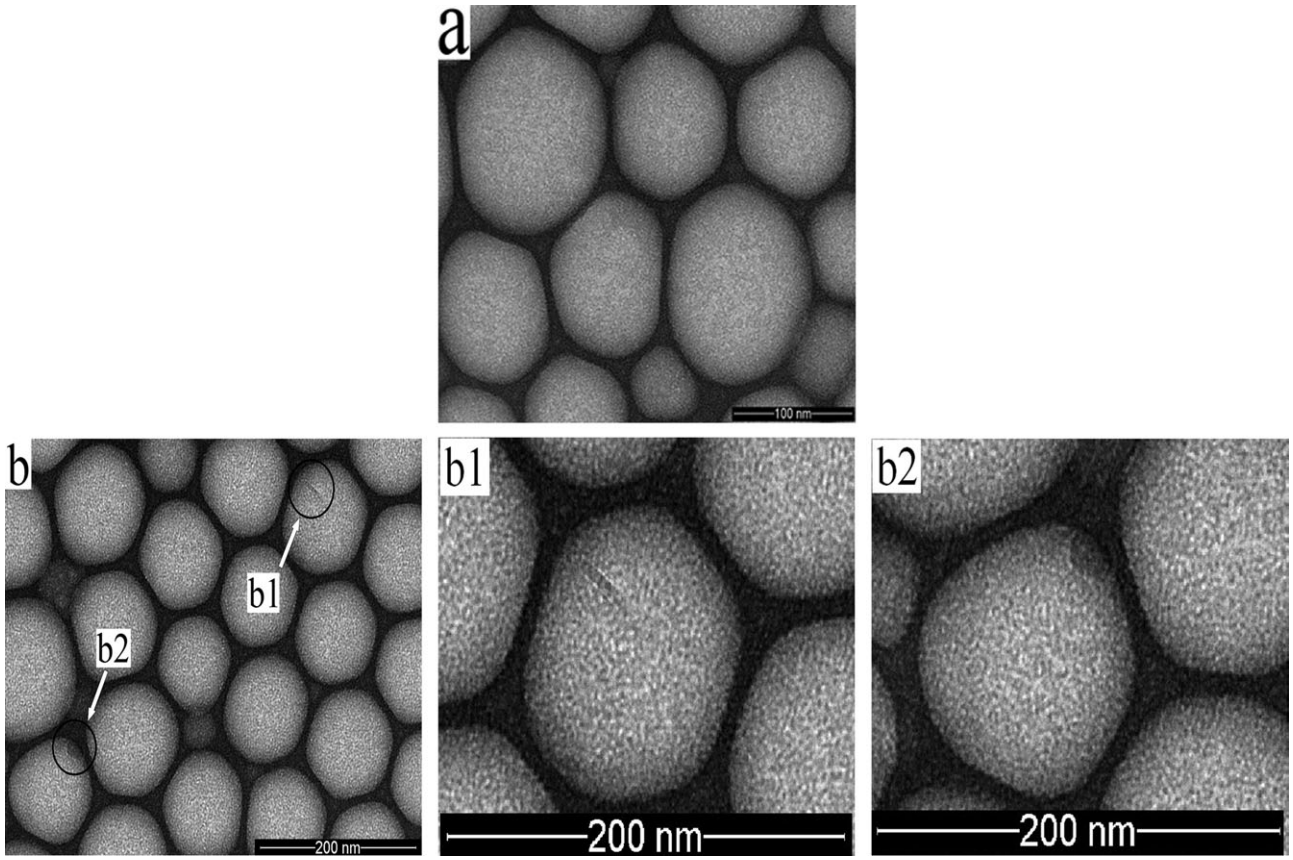


**Figure 7.** TEM images of (a) PBA-3%LRD latexes, (b) PBA-3%LRD-Si latexes and two enlarged images of b. The laponite content in the latexes is 3 wt %.

Applied Polymer SCIENCE

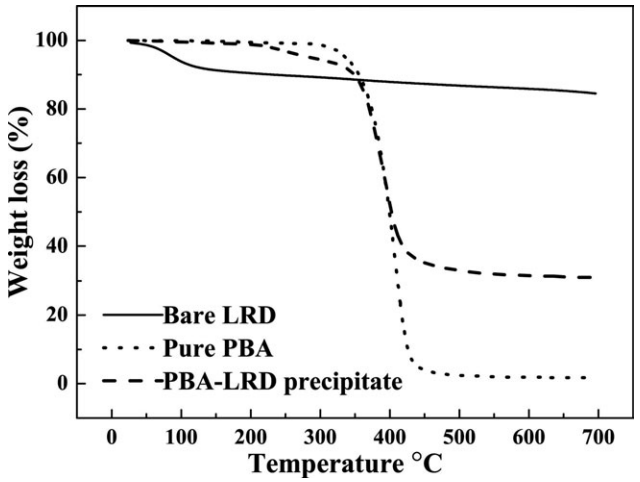


**Figure 8.** TGA traces of the bare LRD, pure PBA and PBA-3%LRD precipitate obtained from the miniemulsion polymerization. The initial amount of LRD is 0.6 g and that of the precipitate after the polymerization is 0.9 g.

7(b) correspond to LRD-Si platelets. Individual LRD platelets are disk-like, with a lateral diameter of 13–30 nm and a thickness of about 1 nm. From these images, one may infer that some of the latex particles could be exempt of laponite platelets. Nonetheless, the fact that a latex particle appears without black lines or disks cannot necessarily ascertain that it does not contain laponite platelets. This is because the visibility of the laponite under TEM strongly depends on its basal plane orientation. If the latter is perpendicular to the electron beam, the diffraction contrast of the platelet is reduced.

TGA was used to investigate the contents of LRD or LRD-Si in the precipitates after the miniemulsion polymerization. As shown in Table II, the initial amount of BA monomer is 20 g and that of LRD or LRD-Si added is 0.6 g for the preparation of PBA nanocomposite latex. Figures 8 and 9 show the TGA of the PBA latex and that of the precipitates, respectively. Accord-

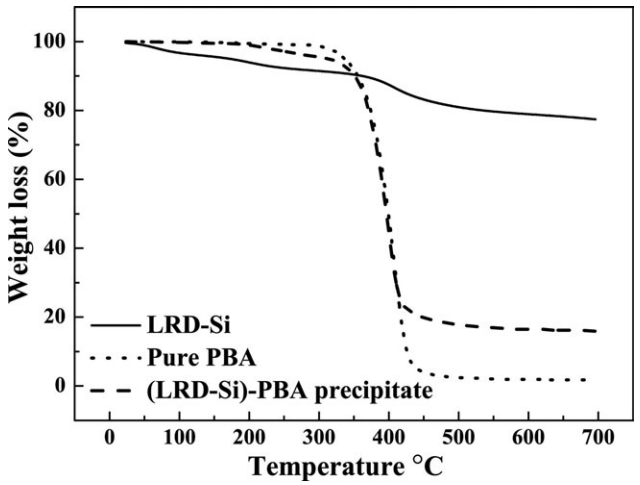


**Figure 9.** TGA traces of the bare LRD-Si, pure PBA and PBA-3%LRD-Si precipitate after miniemulsion polymerization. The initial amount of LRD-Si is 0.6 g and that of the precipitate after polymerization is 0.5 g.

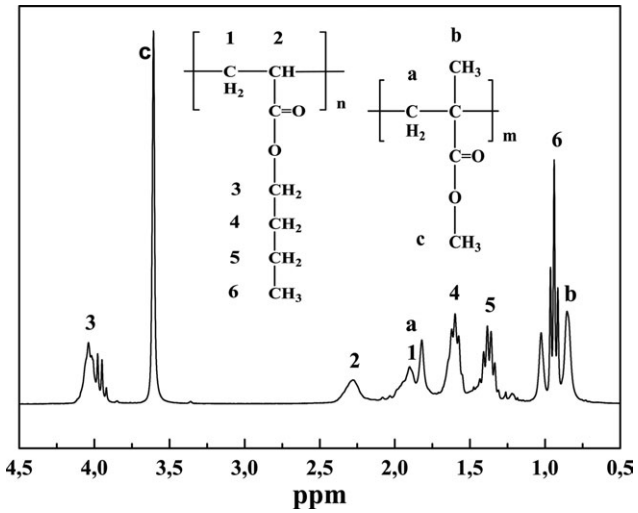


**Figure 10.** $^1$H-NMR spectrum of PBA-PMMA core–shell particles.

ing to Figure 8, the amount of the LRD in the precipitate after the miniemulsion polymerization is about 0.3 g. This means that only 50% of the LRD is incorporated in the PBA latex, even though CTAB is used as a surfactant. Conversely, according to Figure 9, 85% of LRD-Si is incorporated in the PBA latex.

The above results show that the use of a cationic surfactant such as CTAB allows obtaining PBA-LRD and PBA-LRD-Si latexes. As a matter of fact, the silane-grafted LRD-Si nanoparticles are well suspended in the miniemulsion of BA monomer and a high percentage of them are incorporated in the PBA latex particles after the polymerization. This is because the silane molecules on the LRD-Si nanoparticles can react with the BA monomer during the polymerization.

### Synthesis and Characterization of Core PBA-shell PMMA Latexes

Considering that PBA and PLA are immiscible, PBA-MMA core–shell latexes with or without LRD (or LRD-Si) were prepared by seeded emulsion polymerization in order to improve compatibility between nanoparticles and matrix (The PMMA shell, is miscible with PLA matrix). Core–shell nanoparticles were characterized by $^1$H-NMR and TEM. PBA latexes with or without LRD (or LRD-Si) were used as seeds ("Experimental" Section). MMA was polymerized in the presence of these seeds in order to obtain PBA-PMMA core–shell particles. The feed rate of the MMA monomer was kept constant and under starved conditions so that the seed latex particles had enough time to polymerize with MMA, thus preventing the second generation of PMMA particles. The BA/MMA ratio was about 50/50 (w/w) to obtain well-defined core–shell structures.[28]

Figure 10 shows the $^1$H-NMR spectra of PBA-PMMA latexes. The peak at 3.6 ppm (c) and multiple peaks at 4.0 ppm (3) correspond to the O—$CH_2$ of the PBA and O—$CH_3$ of the PMMA, respectively. The peaks between 0.8 and 2.0 ppm can be ascribed to the overlapping between protons. The composition of the PBA and PMMA was calculated by integrating the $OCH_2$ protons of PBA (3) and the $OCH_3$ protons of PMMA (c), giving a PBA/PMMA weight composition equal to 51/49 (w/w).[29]

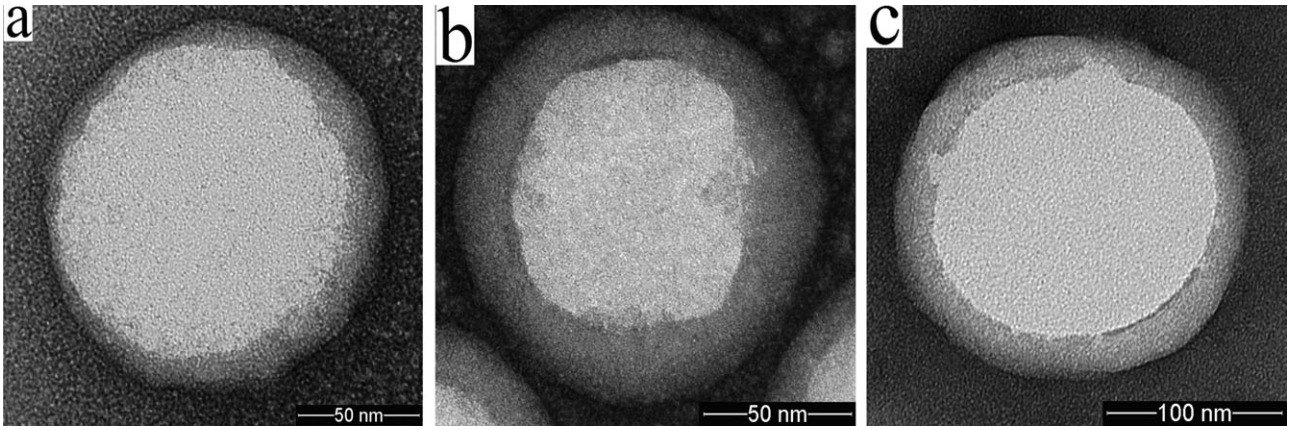


**Figure 11.** TEM images of PBA-PMMA core–shell particles. (a) PBA-PMMA, (b) (PBA-3%LRD)-PMMA, and (c) (PBA-3%LRD-Si)-PMMA.

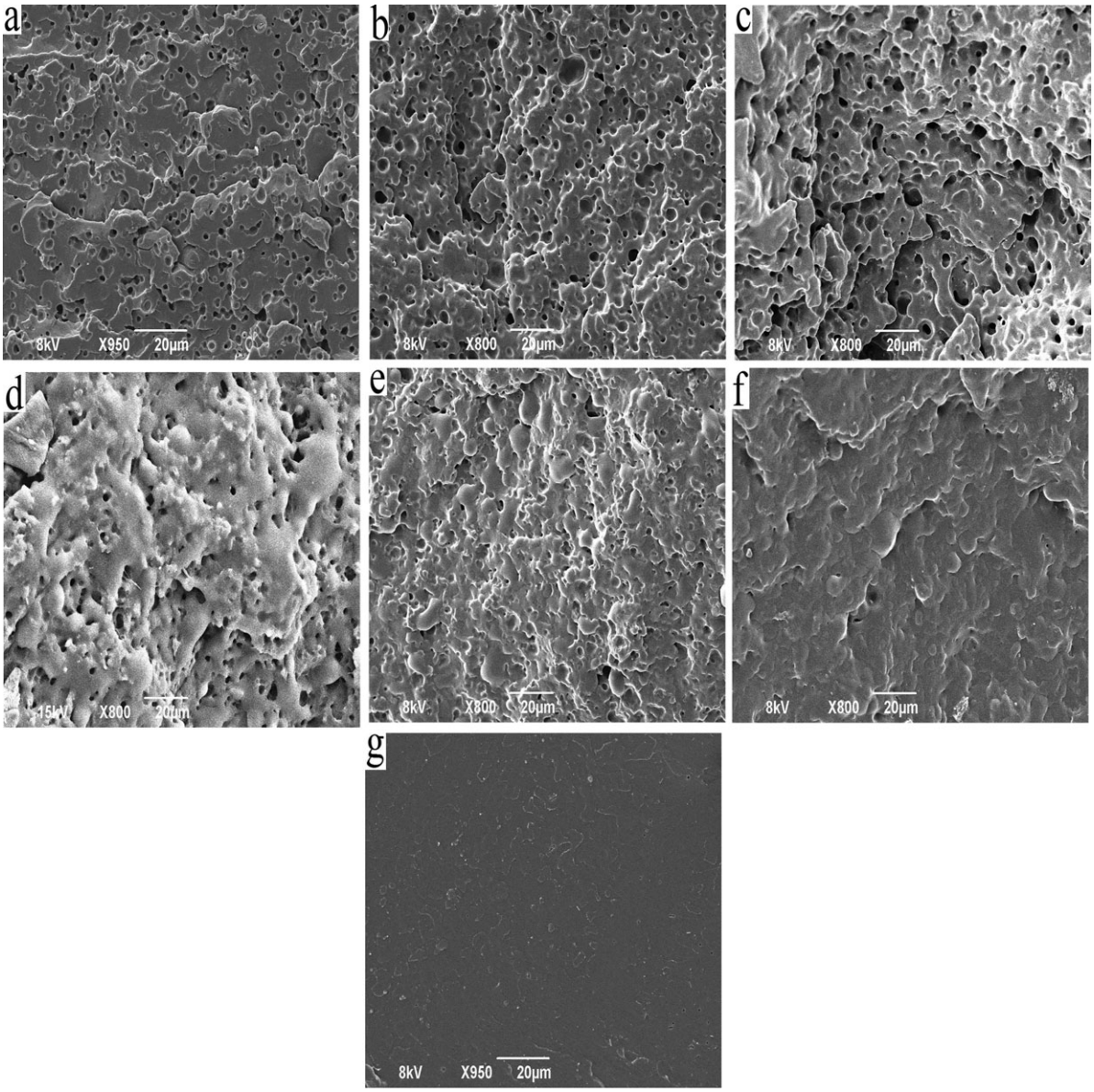


**Figure 12.** SEM images of (a) PBA/PLA (10/90) blend, (b) PBA/PLA (20/80) blend, (c) PBA-3%LRD/PLA (20/80) blend, (d) PBA-2%LRD-Si/PLA (20/80) blend, (e) PBA-3%LRD-Si/PLA (20/80) blend, (f) PBA-5%LRD-Si/PLA (20/80) blend, and (g) pure PLA.

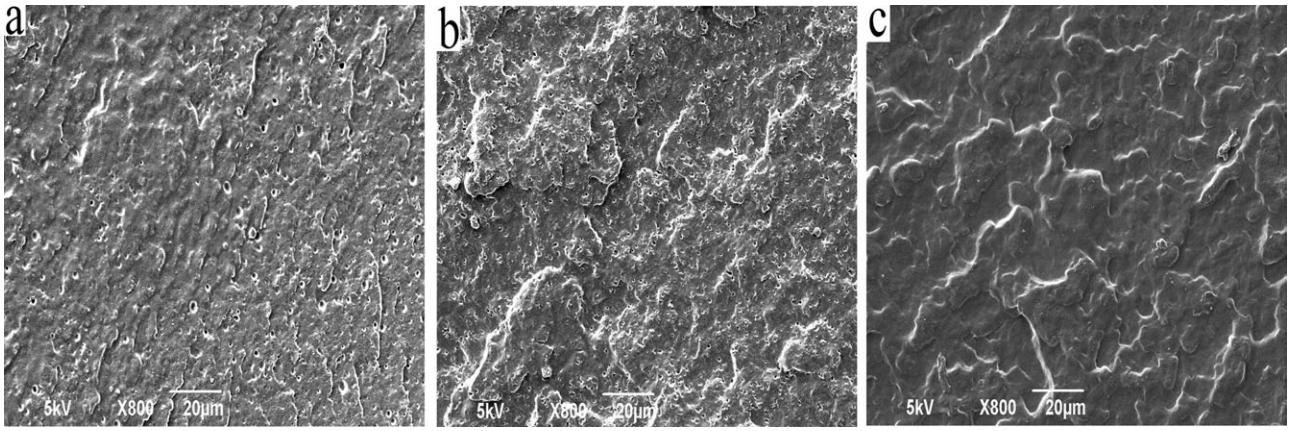


**Figure 13.** SEM micrographs of freeze-fractured surfaces of (a) (PBA-PMMA)/PLA, (b) (PBA-3%LRD-PMMA)/PLA, and (c) (PBA-3%LRD-Si-PMMA)/PLA blends.

Figure 11 shows the TEM images of the PBA-PMMA core–shell particles. The soft core in PBA and the hard shell in PMMA are clearly seen. The former covers the latter sufficiently well and uniformly. The thickness of the shell and the diameter of the core are 10–20 and 90–130 nm, respectively. This is also consistent with the compositions of PBA and PMMA in the core–shell particles.

### Morphology of PBA/PLA and (PBA-PMMA)/PLA Blends

Figure 12 shows the SEM images of the PBA/PLA (10/90), PBA/PLA (20/80), PBA-3%LRD/PLA (20/80), PBA-2%LRD-Si/PLA (20/80), PBA-3%LRD-Si/PLA (20/80), and PBA-5%LRD-Si/PLA (20/80) blends together with that of the pure PLA. Prior to the SEM analyses, the surfaces of these materials are etched with 2-butanol, a good solvent of PBA and a nonsolvent for the PLA. The surfaces of the PBA/PLA (10/90), PBA/PLA (20/80), and PBA-3%LRD/PLA (20/80) blends exhibit holes while the surfaces of the three PBA-LRD-Si/PLA (20/80) blends (d)–(f) trend to be smooth. Concerning the average diameter of the holes in these blends which corresponds to the etched PBA domains, it is about 1, 1.8, 1.8, 1.6, and 1.4 $\mu$m for blends (a), (b), (c), (d), and (e), respectively. As for blend (f) which contains 5%LRD-Si, there are almost no holes on the surface after etching, confirming that the PBA-LRD-Si particles are crosslinked during the miniemulsion polymerization by the MPTMS grafted LRD-Si. The degree of crosslinking is enhanced with increasing LRD-Si content. Meanwhile, the values of these holes in the blends are significantly higher than the average diameter of the PBA nanoparticles recovered from miniemulsion polymerization. This implies that they are likely agglomerated during the drying stage of the latexes before blending with the PLA. Agglomeration during the melt blending could also be possible.

Figure 13 shows the SEM images of (PBA-PMMA)/PLA (10/10/80), (PBA-3%LRD-PMMA)/PLA (10/10/80), and (PBA-3%LRD-Si-PMMA)/PLA (10/10/80) blends. Their surfaces are etched with 2-butanol prior to the SEM analyses. Holes of about 350 nm in diameter are observed on the surfaces of the first two blends, keeping in mind that the diameter of the original PBA-PMMA core–shell particles is around 125 nm after the emulsion polymerization. The fact that these holes are much smaller than those in the PBA/PLA blends implies that the PMMA shell does play a role of compatibilization between PBA and PLA. This strongly improves the dispersion of nanoparticles

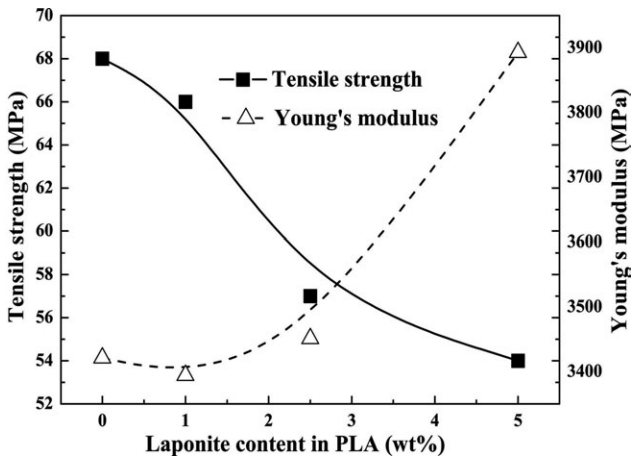


**Figure 14.** Effects of the incorporation of the LRD on the tensile strength and Young's modulus of the PLA.

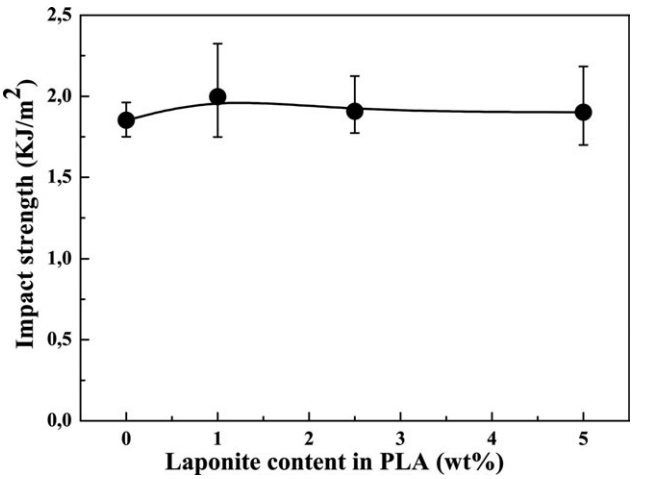


**Figure 15.** Effect of the incorporation of the LRD on the impact strength of the PLA.

Table V. Tensile Strength, Young's Modulus, and Impact Strength of the Pure PLA, PBA/PLA Blends, and PBA/PMMA/PLA Blends

| Blends | Tensile strength (MPa) | Young's modulus (MPa) | Impact strength (KJ/m$^2$) |
|---|---|---|---|
| PLA | 68 | 3421 | 1.85 |
| PBA/PLA | 37 | 2061 | 2.39 |
| (PBA-2%LRD-Si)/PLA | 33 | 2307 | 3.99 |
| (PBA-5%LRD-Si)/PLA | 33 | 2105 | 4.50 |
| PBA-PMMA/PLA | 51 | 2607 | 5.69 |
| (PBA-2%LRD-Si-PMMA)/PLA | 52 | 2620 | 5.78 |
| (PBA-5%LRD-Si-PMMA)/PLA | 47 | 2703 | 5.24 |
| (PBA-5%LRD-PMMA)/PLA | 50 | 2565 | 5.51 |

in the PLA matrix. There are no holes on the surface of the (PBA-3%LRD-Si-PMMA)/PLA (10/10/80) blend. This is because in this blend, the PBA core is crosslinked by the silane grafted LRD (LRD-Si) and cannot be etched by 2-butanol.

**Mechanical Properties**

**PLA/LRD Blends.** PLA/LRD blends were prepared for the sake of comparison with the other PLA blends prepared in this work. Figure 14 shows that the Young's modulus of the PLA increases with increasing LRD load. However its tensile strength decreases significantly. From Figure 15, the impact strength of the PLA is very low and is not affected much by the incorporation of the LRD.

**PBA/PLA and (PBA-PMMA)/PLA Blends.** Table V shows the Izod impact strength and the tensile properties of the PBA/PLA and (PBA-PMMA)/PLA blends.

As expected, the incorporation of the PBA to the PLA decreases its tensile strength and Young's modulus by about 50 and 36%, respectively. Nevertheless, the type of the PBA composite does not affect much their tensile properties. Its impact strength is improved to a noticeable extent.

When PBA-LRD or PBA-LRD-Si nanocomposite nanoparticles are incorporated in the PLA, its impact strength is increased by 55–88% with respect to the pure PBA nanoparticles without LRD or LRD-Si. The effect of the PBA-LRD-Si is even slightly stronger than that of the LRD.

When PBA-PMMA core–shell particles with or without LRD or LRD-Si are incorporated in the PLA, both the tensile properties and impact strength are largely improved with respect to their PBA analogues. This further confirms the importance of the PMMA shell which not only has a higher Young's modulus than PBA but also ensures better compatibility with the PLA.

## CONCLUSIONS

This work developed a miniemulsion polymerization methodology to synthesize PBA-PMMA core–shell latexes which were subsequently incorporated in PLA in order to improve its impact strength without significantly reducing its tensile properties. The incorporation of the PBA nanoparticles in the PLA increased the impact strength of the PLA while significantly reducing its tensile strength and Young's modulus. When laponite was incorporated in the PBA nanoparticles, the Young's modulus of the PLA blends was further improved. When the PBA-laponite nanocomposite nanoparticles were encapsulated by PMMA shell which not only had better tensile properties than but also better compatibility with the PLA, the impact strength of the resulting (PBA-LRD-PMMA)/PLA blends was significantly higher than that of the PLA, with a minimum decrease in tensile strength and their Young's modulus. With the improved impact strength obtained, the modified PLA can be used for packaging applications including containers, overwrap and bags.

## REFERENCES


1. Yongjin Li, Hiroshi Shimizu. *Eur. Polym. J.* **2009**, *45*, 738.
2. Su, Z.; Li, Q.; Liu, Y.; Hu, G.-H.; Wu, C. *Eur. Polym. J.* **2009**, *45*, 2428.
3. Balakrishnan, H.; Hassan, A.; Wahit, M. U.; Yussuf, A. A.; Razak. S. B. A. *Mater. Des.* **2010**, *31*, 3289.
4. Qin, L.; Qiu, J.; Liu, M.; Ding, S.; Shao, L.; Lu, S.; Zhang, G.; Zhao, Y.; Fu, X. *Chem. Eng. J.* **2011**, *166*, 772.
5. Ishida, S.; Nagasaki, R.; Chino, K.; Dong, T.; Inoue, Y. *J. Appl. Polym. Sci.* **2009**, *113*, 558.
6. Murariu, M.; Da Silva Ferreira, A.; Degee, P. *Polymer* **2007**, *48*, 2613.
7. Murariu, M.; Da Silva Ferreira, A.; Pluta, M.; Bonnaud, L. Alexandre, M.; Dubois, P. *Eur. Polym. J.* **2008**, *44*, 3842.
8. Shi, D.; Yu, W.; Li, R. K. Y. *J. Mater. Sci.* **2008**, *43*, 1162.
9. Chow, W. S.; Lok, S. K. *J. Thermal Anal. Calorim.* **2009**, *95*, 627.
10. Yu, Z.-Z.; Hu, G.-H.; Varlet, J.; Dasari, A.; Mai, Y.-W. *J. Polym. Sci. Part B: Polym. Phys.* **2005**, *43*, 1100.
11. Negrete-Herrera, N.; Putaux, J.-L.; David, L.; De Haas, F. *Macromol. Rapid Commun.* **2007**, *28*, 1567.
12. Putlitz, B. Z.; Landfester, K.; Fischer, H.; Antonietti, M. *Adv. Mater.* **2001**, *13*, 500.
13. Bourgeat-Lami, E. *J. Nanosci. Nanotechnol.* **2002**, *2*, 1.
14. Sun, Q.; Deng, Y.; Wang, Z. L. *Macromol. Mater. Eng.* **2004**, *289*, 288.
15. Negrete-Herrera, N.; Putaux, J. L.; David, L.; Bourgeat-Lami, E. *Macromolecules* **2006**, *39*, 9177.
16. Ruggerone, R.; Plummer, C. J. G.; Negrete-Herrera, N.; Bourgeat-Lami, E.; Jan-Anders, E. *Eur. Polym. J.* **2009**, *45*, 621.
17. Voorn, D. J.; Ming, W.; van Herk, A. M. *Macromolecules* **2006**, *39*, 4654.
18. Negrete-Herrera, N.; Letoffe, J.-M.; Putaux, J.-L.; David, L.; Bourgeat-Lami, E. *Langmuir* **2004**, *20*, 1564.
19. Negrete-Herrera, N.; Letoffe, J.-M.; Reymond, J.-P.; Bourgeat-Lami, E. *J. Mater. Chem.* **2005**, *15*, 863.
20. Negrete-Herrera, N.; Putaux, J.-L.; Bourgeat-Lami, E. *Prog. Solid State Chem.* **2006**, *34*, 121.

21. Wang, T.; Wang, M.; Zhang, Z.; Ge, X.; Fang, Y. *Mater. Lett.* **2006**, *60*, 2544.
22. Avella, M.; Errico, M. E.; Immirzi, B.; Malinconico, M.; Martuscelli, E.; Paolillo, L.; Falcigno, L. *Die Angewandte Makromolekulare Chemie* **1997**, *246*, 49 (Nr. 4275).
23. Avella, M.; Errico, M. E.; Immirzi, B.; Malinconico, M.; Falcigno, L.; Paolillo, L. *Macromol. Chem. Phys.* **2000**, *201*, 1295.
24. Zhang, G.; Zhang, J.; Wang, S.; Shen, D. *J. Polym. Sci. Part B: Polym. Phys.* **2003**, *41*, 23.
25. Eguiburu, J. L.; Fernandez-Berridi, M. J.; San Roman, J. *Polymer* **1996**, *37*, 3615.
26. G'Sell, C.; Hiver, J. M.; Dahounet, A.; Souahi, A. *J. Mater. Sci.* **1992**, *27*, 5031.
27. Gaikwad, A. N.; Wood, E. R. *Macromolecules* **2008**, *41*, 2502.
28. Kirsch, S.; Pfau, A.; Landfester, K.; Shaffer, O.; El-Aasser, M. S. *Macromol. Symp.* **2000**, *151*, 413.
29. Wootthikanokkhan, J.; Burford, R. P.; Chaplin, R. P. *J. Appl. Polym. Sci.* **1996**, *62*, 835.